Infrared Subpicosecond Laser Pulses with a Free-Electron Laser

F. Glotin, R. Chaput, D. Jaroszynski, R. Prazeres, and J.-M. Ortega
Laboratoire pour l'Utilisation du Rayonnement Electromagnetique, Bâtiment 209D, Université Paris-Sud, 91405 Orsay CEDEX, France
(Received 8 July 1993)

Subpicosecond laser pulses (down to 200 fs) have been produced and measured with a free-electron laser oscillator at a wavelength around 8.5 μm. This has been achieved by running our linear accelerator in a configuration where the electron bunches acquire a quasilinear time-energy relationship while traveling on the side, rather than on the crest, of an accelerating high-frequency wave.

PACS numbers: 41.60.Cr, 42.65.Re, 42.60.−v

In the last decade there have been important developments of the so-called free-electron laser (FEL), and in particular several infrared user facilities are operating throughout the world [1].

FEL's driven by rf accelerators provide short laser pulses, due to their pulsed electron beam structure. Usually pulses are a few picoseconds long (FWHM), with a peak power in the megawatt range. They are dedicated to various experiments involving nonlinear phenomena and fast kinetic processes with high temporal resolution. These features, combined with the continuous tunability in wavelength of the FEL, provide a very useful tool to scientists in many fields [1–5]. The laser wavelength is given by

$$\lambda_L \cong (\lambda_0/2\gamma^2)(1+0.44B_0^2\lambda_0^2)\,, \qquad (1)$$

where λ_0 is the period in the lab frame of the magnetic field generated by the so-called "undulator" magnet, γ is the relativistic factor of the electrons, and B_0 the peak intensity of the on-axis magnetic field.

CLIO (Collaboration for an Infrared Laser at Orsay) is one such new light source dedicated to applications in the infrared [6–8]. Most users belong to solid state and surface physics, as our present spectral range spans from 2.5 to 17 μm [2–4].

The purpose of this paper is to describe a new and simple method which allows one to produce tunable subpicosecond pulses. In this scheme we do not use any dispersive elements to provide optical pulse compression as previously proposed by various authors [9–13]. However, we have also tried this method, but found that it does not lead to further compression.

The CLIO FEL mainly consists of an S-band linear rf accelerator, an electron transport system, and an optical cavity. The linac consists of an electron gun followed by a pulse-compression stage and a traveling-wave section accelerating a train of short electron bunches up to 70 MeV. A dipole magnet and collimating slit combination allow energy selection of the electrons. The optical cavity (of length such that electron bunches and laser pulses overlap), surrounds a 4 cm period, 1.92 m long planar undulator. The laser beam is extracted with a 3 mm thick ZnSe plate at 60° incidence.

The normal accelerator settings produce electrons which travel through the accelerating section with a phase relative to the 3 GHz rf wave, that optimizes their final energy and energy dispersion. This phase corresponds to the crest of the wave. The optical pulse length then depends on the desynchronism between the optical pulses in the cavity and the electron bunches. Because of the difference between the speed of light and the speed of the electrons, the optimal cavity length for laser buildup is shorter than $L_0=c\tau_e/2$ (where τ_e is the interval between successive bunches) [14,15]. At saturation, the laser properties depend strongly on δL: At short δL (small detuning) the laser power is a maximum, the optical pulse length is a minimum (about 2 ps in our case), and the linewidth is large (1%–2% for CLIO). As δL is increased, the pulse length becomes longer (up to 6–7 ps) and the laser linewidth is decreased. Measurements were performed with a Michelson interferometer and a frequency-doubling crystal, providing second-order intensity autocorrelation curves [16].

Simultaneous recording of the frequency spectrum showed that in both cases the spectral width is approximately Fourier transform limited; i.e., the relation $\delta\omega\delta\tau \approx 2\pi$ is always valid, where $\delta\omega$ and $\delta\tau$ are the FWHM of the frequency spectrum and of the temporal pulse width, respectively. Indeed, the measured spectral FWHM varies between $\Delta\lambda/\lambda = 1.5\%$ for the shortest pulses and 0.4% for the longest ones [7]. In practice, as the pulse temporal shape is not Gaussian (as shown below) the spectra are not Gaussian either and sometimes exhibit complicated structures.

Another accelerator adjustment has been used on CLIO which results in a shortening effect on the laser pulse. By dephasing the rf wave relative to the electron bunch in the accelerator section, the bunch can be made to accelerate off the crest of the accelerating wave. For electrons arriving in advance of the crest, the gain in energy will be reduced and, in addition, the electron bunch will acquire an energy slope such that electrons at the start of the bunch will have a lower energy than the later ones (Fig. 1). As 1° in phase at 3 GHz corresponds roughly to 1 ps and the bunches are 8 to 12 ps long (FWHM), this energy slope will be approximately linear

0031-9007/93/71(16)/2587(4)$06.00

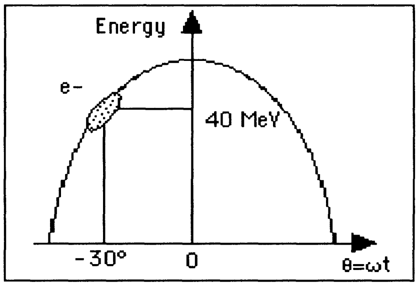

FIG. 1. Schematic of an electron bunch dephased by 30° relative to the 3 GHz accelerating wave.

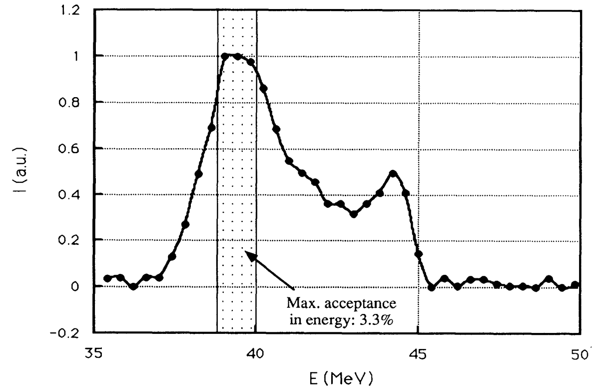

FIG. 2. Experimental energy spectrum in the dephased configuration.

for a bunch dephased by 30° from the crest of the wave. The electrons enter the accelerating section where they are already relativistic as the bunching stage of the machine provide them with an energy of 3 MeV. Thus, the bunch shape is not altered significantly by its travel through the accelerating section. After dispersion by the first dipole magnet, the beam is collimated by the slit. Because of the energy slope, selecting an energy range in the bunch leads to selection of a temporal window as well. Indeed, shorter bunches will be produced by closing the slit. Finite emittance and nonisochronicity of the deviation for particles of different momentum (-0.9 ps/%) must be taken into account to estimate the final bunch length. For a fully opened slit (60 mm), acceptance in energy of the deviation is $\delta\gamma/\gamma=3.3\%$, leading to a 6 ps long bunch. This length is computed by electron beam optics calculations to first order [17].

A measured energy spectrum in this configuration is shown in Fig. 2. Since the electron bunch is wide enough to cover the crest of the HF wave, there are two peaks on such a spectrum. The smallest one is not "real," and is only due to the nonlinearity of the phase-energy relation at the sine crest: Here, a given small window in phase will correspond to a larger energy window than on the sine side. More electrons will then be recorded at this energy for a given slit width. In Fig. 2, the peak energy is 44.2 MeV, the central energy for the electron bunch is 39.4 MeV, thus the phase shift is 28° for an input energy of 3 MeV in the accelerating section.

As the laser wavelength varies as $(2\gamma^2)^{-1}$, it has been suggested that such special electron bunches would lead to laser pulses chirped in wavelength [9–13]. These pulses could thereafter be time compressed using dispersive devices, following the usual methods for femtosecond pulse generation with conventional lasers. Experimental verification has been attempted on CLIO at 8.5 μm with a pair of gratings (75 lines/mm, blazed at 9 μm). The accelerator configuration was the one described above, with a central energy of 40 MeV for the electron bunches after they were dephased by 30° relative to the rf wave. After two passes of the optical pulses through the grating pair, intensity autocorrelation measurements were carried out, averaging over the whole laser macropulse. This resulted in no evidence of pulse compression, as the same autocorrelation curves could be produced by omitting the gratings from the experimental setup. Modification of the distance between gratings (i.e., compression ratio) did not modify the nonlinear signal, indicating no change of the laser peak power and consequently, of its pulse width.

Indeed, we have studied the development of such optical pulses with simulations, using a multiparticle code to solve the Maxwell-Lorentz equations in the so-called "slowly varying approximation" [11,14,15]. We find, as in Refs. [11,12], that at small signal level the optical pulses exhibit the expected chirping in wavelength. But as the optical power grows, the frequency-time relationship inside the main laser pulse becomes distorted due to saturation processes, leading to pulses unsuitable for compression techniques.

Measurement at small signal level was not possible because of the sensitivity of the frequency doubling crystal used in the measurements, and pulse compression at small signal levels would not be very useful anyway because of the much smaller peak power.

Interestingly, even without frequency chirping it appears that running the linac in the dephased setup allows one to produce substantially shorter laser pulses, by at least a factor of 2 (Fig. 3). It is difficult to find a fundamentally pertinent parameter with which to compare different pulse lengths, as pulse shapes can vary greatly according to different laser conditions. The assumption of a Gaussian profile allows an easy deconvolution but can rarely be used confidently as evidence of sharp spikes in the temporal structure occurs most of the time. This "spiking" behavior is not surprising as it is a well-known feature of the FEL physics. When the laser power in the cavity becomes high enough, electrons experience small longitudinal oscillations in the periodic ponderomotive potential resulting from the combination of the laser light and the undulator magnet electromagnetic fields. These so-called "synchrotron oscillations" modulate both the

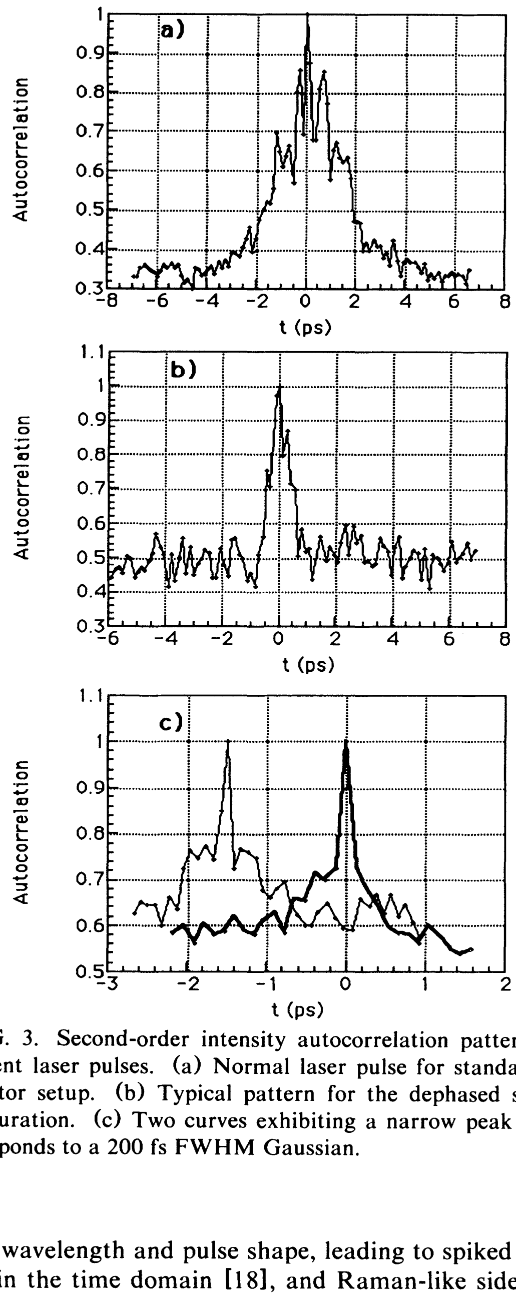

FIG. 3. Second-order intensity autocorrelation patterns for different laser pulses. (a) Normal laser pulse for standard accelerator setup. (b) Typical pattern for the dephased section configuration. (c) Two curves exhibiting a narrow peak which corresponds to a 200 fs FWHM Gaussian.

laser wavelength and pulse shape, leading to spiked structure in the time domain [18], and Raman-like sidebands on the frequency spectrum. These modulations tend to be enhanced with time, as they grow in an unstable manner [14,15].

However, the shortening effect of the dephased configuration clearly appears when one looks at the overall autocorrelation patterns. These curves exhibit an approximate FWHM for normal laser pulses of about 2 ps, and 1 ps or less in the dephased setup. We can define a FWHM by assuming some mathematical form to the optical pulse. This correction factor varies for most assumed pulse shapes, typically between 0.7 (Gaussian) and 0.4 (symmetric two-sided exponential). The Gaussian hypothesis gives a 700 fs FWHM for the typical short pulse shown in Fig. 3(b), and other assumptions lead to less than 500 fs FWHM.

Some autocorrelation curves are shown in Fig. 3, for both a normal pulse [3(a)] and dephased (shortened) ones [3(b) and 3(c)]. All of them are time averaged over the macropulse duration, which is 10 μs long. Figure 3(a) shows a net pulse substructure with at least three spikes, but the whole pulse still presents a FWHM of 2 ps in the Gaussian assumption. Such a regular spiked structure constitutes evidence in the time domain of some frequency modulation due to synchrotron oscillations [14,18]. Figure 3(b) corresponds to a dephased short pulse without clear evidence of substructure, and can be seen as a good example of a "Gaussian" 700 fs FWHM pulse. This pulse width is reproducible without difficulties. Both curves in Fig. 3(c) exhibit a very narrow peak, corresponding to a 200 fs FWHM Gaussian. On the first curve (left one), there is also a second peak, indicative of a more complicated structure. Whereas the second curve (right one) is quite simple, and shows how short a pulse can be when there is no development of a substructure. These curves correspond to the shortest pulses observed.

In practice, the method is quite simple to operate. We expect that it will allow kinetics with resolution better than 1 ps, and this will be tested soon on real systems.

We have lased with shorter electron bunches obtained by closing the slit, but no effect was observed on the laser pulse width, even with a 3 times shorter bunch. The laser pulse shortening must then originate from the temporal energy slope in the electron bunches rather than from the shortening of the electron pulse. The origin of this effect is not yet clear. We can remark that the energy slope induces a large spread in the emitted wavelengths. As the laser linewidth becomes larger, the corresponding pulse width will become smaller if we remain in the transform limited regime. In fact, it seems that the shortening effect results mainly from an attenuation of the spiked substructure in the laser pulse. As the laser pulse slip over the electrons while traveling down the undulator due to their different velocities, a given part of the pulse will experience different values of gain for different positions of the laser pulse relative to the electron bunch. This must affect the sideband development in the saturated regime, and hamper correspondingly the growth of the secondary peaks in the time domain. Numerical simulations are under way to understand the details of this process. These experiments have been performed at a wavelength around 8.5 μm. It is likely that the same effect will occur at other wavelengths. Experiments in the CLIO wavelength range (2.5–17 μm) are in progress.

[1] *Proceedings of the XIVth International FEL Conference, Kobe, 1992* [Nucl. Instrum. Methods Phys. Res., Sect. A **311** (1993).

[2] B. N. Murdin *et al.*, Opt. Quantum Electron. **25**, 171 (1993).

[3] D. Jaroszynski *et al.*, Nucl. Instrum. Methods Phys. Res., Sect. A **311**, 640 (1993).

[4] A. Peremans *et al.*, Nucl. Instrum. Methods Phys. Res., Sect. A **311**, 28 (1993).

[5] Special issue on FEL Applications, J. Opt. Soc. Am. **6**, No. 65, 972–1089 (1989).

[6] R. Chaput *et al.*, Nucl. Instrum. Methods Phys. Res., Sect. A **311**, 267 (1993).

[7] R. Prazéres *et al.*, Nucl. Instrum. Methods Phys. Res., Sect. A **311**, 15 (1993).

[8] F. Glotin *et al.*, in *Proceedings of the IIIrd European Particle Accelerator Conference, Berlin, 1991* (Editions Frontieres, Gif-sur-Yvette, 1992).

[9] G. T. Moore, Phys. Rev. Lett. **60**, 1825 (1988).

[10] G. T. Moore, Nucl. Instrum. Methods Phys. Res., Sect. A **272**, 302 (1988).

[11] G. T. Moore and J. C. Goldstein, Nucl. Instrum. Methods Phys. Res., Sect. A **285**, 176 (1989).

[12] E. B. Szarmes *et al.*, Nucl. Instrum. Methods Phys. Res., Sect. A **296**, 755 (1990).

[13] E. B. Szarmes *et al.*, Nucl. Instrum. Methods Phys. Res., Sect. A **318**, 914 (1992).

[14] C. A. Brau, *Free-Electron Lasers* (Academic, San Diego, 1990).

[15] *Laser Handbook*, edited by W. B. Colson, C. Pellegrini, and A. Renieri (North-Holland, Amsterdam, 1990), Vol. 6.

[16] J. A. Armstrong *et al.*, Appl. Phys. Lett. **10**, 16 (1967).

[17] TRANSPORT, a computer program for designing charged particle beam transport system, in K. L. Brown *et al.*, CERN Report No. 80-04 (unpublished).

[18] B. A. Richman *et al.*, Phys. Rev. Lett. **63**, 1683 (1989).